Wall Deadlock Evasion Control Based on Rotation Radius Adjustment

Shotaro Kojima, Kazunori Ohno, Takahiro Suzuki, Yoshito Okada, Thomas Westfechtel, and Satoshi Tadokoro

***Abstract*—This letter describes a wall deadlock evasion method for tracked vehicles. Wall deadlock is a phenomenon where the robot cannot rotate to the commanded direction when it collides with a wall, because the motion is restricted by the wall. The key idea behind solving this problem involves an adjustment of the rotation radius to generate sufficient rotational moment. There are several approaches to generate a rotational moment; however, no previous solution has been established to address this problem by adjusting the rotation radius based on the dynamics of wall deadlock. In this letter, the authors propose a new wall deadlock evasion method based on the sufficient rotation radius estimation. Experimental results show that the robot can generate rotational motion that satisfies conditions expected by the model. The wall deadlock evasion method is implemented and shows improved performance in terms of reproducibility of motion compared with the different approach proposed in our previous work. Wall deadlock evasion provides more choices of motion such as being as close to the obstacles as possible and ensures that the robot can continue locomotion after such motion. By handling wall deadlock, the robots can utilize surrounding walls for motion in situations such as relative positioning or driving in fixed lanes.**

***Index Terms*—Motion control, autonomous vehicle navigation, dynamics, wheeled robots.**

I. Introduction

This paper describes a wall deadlock evasion method for tracked vehicles. Wall deadlock is a phenomenon where the robot cannot rotate to the commanded direction when it collides with a wall, because the motion is restricted by the wall. This problem is often encountered when the vehicle navigates in narrow corridors such as in industrial plant inspection tasks.

Manuscript received September 10, 2019; accepted January 2, 2020. Date of publication January 17, 2020; date of current version February 3, 2020. This letter was recommended for publication by Associate Editor Y. Pan and Editor D. Popa upon evaluation of the reviewers' comments. This work was supported by CREST Recognition, Summarization and Retrieval of Large-Scale Multimedia Data. *(Corresponding author: Shotaro Kojima.)*

S. Kojima, T. Westfechtel, and S. Tadokoro are with the Graduate School of Information Science, Tohoku University, Sendai 980-8579, Japan (e-mail: kojima@rm.is.tohoku.ac.jp; thomas@rm.is.tohoku.ac.jp; tadokoro@rm.is.tohoku.ac.jp).

K. Ohno is with the New Industry Creation Hatchery Center, NICHe Tohoku University, Sendai 980-8579, Japan, and also with the RIKEN Center for Advanced Intelligence Project, Tokyo 103-0027, Japan (e-mail: kazunori@rm.is.tohoku.ac.jp).

T. Suzuki is with the New Industry Creation Hatchery Center, NICHe Tohoku University, Sendai 980-8579, Japan (e-mail: suzukitk@iis.u-tokyo.ac.jp).

Y. Okada is with the RIKEN Center for Advanced Intelligence Project, Tokyo 103-0027, Japan (e-mail: okada@rm.is.tohoku.ac.jp).

This letter has supplementary downloadable material available at https://ieeexplore.ieee.org, provided by the authors.

Digital Object Identifier 10.1109/LRA.2020.2967332

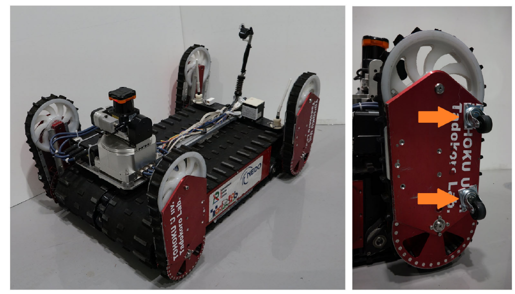

(a) (b)

Fig. 1. Tracked vehicle with sub-tracks "Quince" attached to caster wheels on the side surface.

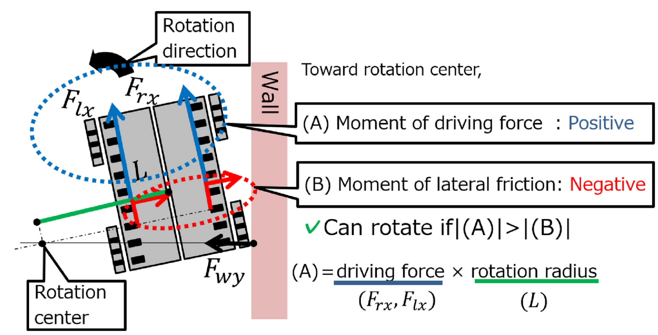

Fig. 2. Overview of wall deadlock problem and its solution. The robot can evade wall deadlock if it generates proper rotational moment to the commanded direction, otherwise it cannot leave the wall.

During plant inspection tasks, the robot needs to pass through a 0.8 m wide passage, although the robot has a width of 0.5 m. It is quite difficult for tracked vehicles to navigate in such a narrow passage because of the small margin for obstacles and positioning error caused by track's slippage during rotation. The amount of slippage also depends on the floor material, which makes it more difficult to estimate or avoid collisions. The authors propose to handle wall deadlock by attaching passive wheels on side surface of the robot as shown in Fig. 1(b) and adjusting motion as shown in Fig. 2.

The key idea of our proposed method is the adjustment of the rotation radius to generate sufficient rotational moment. During the wall deadlock, as shown in Fig. 2, rotational motion is obstructed by the opposite rotational moment generated by the lateral friction of the tracks. To generate rotational motion to the commanded direction, the robot needs to increase the rotational radius or the driving force of both side tracks. The authors aim to adjust rotational radius rather than the driving force, because there is a physical limitation that the driving force

TABLE I

CONDITIONS UNDER WHICH WALL DEADLOCK OCCURS AND THE APPLICATION SCOPE OF SOLUTIONS. THE PROBLEM OCCURS ON TRACKED AND SKID-STEERING VEHICLES WITHOUT EXCEPTION, AND ON DIFFERENTIAL-WHEELED VEHICLES DEPENDING ON THE BODY SHAPE. HOWEVER, THE PROBLEM DOES NOT OCCUR ON ACKERMANN-STEERING AND OMNI-DIRECTIONAL VEHICLES BECAUSE THEY CAN ACTIVELY CHANGE THE DIRECTION OF THE DRIVING FORCE

Vehicle type		Tracked	Skid steering	Differential wheeled	Ackermann steering	Omni directional
		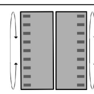	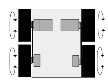	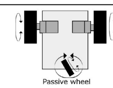	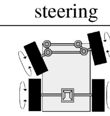	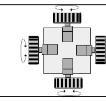
Whether wall deadlock is occurred		✓ Yes	✓ Yes	△ Depends on body shape	× No	× No
Solutions	Wall-deadlock evasion (**proposed**)	✓ Available	✓ Available	✓ Available	-	-
	wall-contacting drive [1]	△ Depends on the environment	△ Depends on the environment	△ Depends on the environment	-	-
	Circular-shaped body [2]	× Not suitable	× Not suitable	✓ Available	-	-
	Shock-absorbing bumper [3]	× Not suitable	× Not suitable	✓ Available	-	-

cannot exceed the maximum friction force. The robot cannot evade wall deadlock by simply increasing the driving force, because wheel slippage is increased when a large driving force is used. On the other hand, there is no physical limitation in the rotational radius. It can be adjusted from zero to infinite by changing the velocity of both side track.

In this letter, the authors construct a wall deadlock evasion method based on the adjustment of rotation radius and implement wall-deadlock evasion motion control. Experimental results show that there is a boundary in motion commands that determines whether the robot can evade wall deadlock, which is expected by our model. The wall deadlock evasion method is implemented, and shows higher performance in reproducibility of motion compared with the different implementation described in our previous work.

The authors aim to utilize collisions for motion by handling wall deadlock. In plant inspection tasks, the robot needs to inspect small targets such as meters or peepholes for combustion confirmation so that high positioning accuracy is required. In such scenarios, positioning accuracy is increased if the robot collides surrounding obstacles such as a wall or a fall prevention plate to adjust its relative position to the target. It is quite natural for human inspectors to touch the wall or handrails during inspection to keep the position. Also, unexpected collision is prevented if the robot follows the wall in a straight passage, because its traveling lane is determined by the wall. This motion is equivalent to human inspectors grasping handrails when they walk in narrow passages or on staircases. Although human inspectors often utilize contact with some objects, it is impossible for tracked vehicles to do the same thing, because of the wall deadlock problem.

The word "wall deadlock," which was originally defined in our previous work [4], is a common problem of several types of robots, and was previously reported on a skid-steering [1], as well as a differential drive [2] vehicles. They noticed that the rotational motion is inhibited by collision, especially when rotating in a small radius. Table I presents wall deadlock occurring conditions. It occurs on non-holonomic vehicles with a differential-steering mechanism, while not on ackermann-steering vehicles and omni-directional vehicles, which can change the direction of driving force while leaving the wall.

Here, the authors developed the wall-deadlock evasion method for the differential-steering vehicles. In principle, it can be utilized not only on tracked vehicles, but also on other differential-steering vehicles, because the modeling and implementation methods well used the related definition in differential-steering vehicles. Moreover, the proposed method does not require major mechanical changes on the vehicle's body compared to the conventional hardware-based approaches.

The authors focus only on tracked vehicles in this study, which are often used for industrial plant inspection tasks due to high mobility, and frequently face the wall deadlock problem during autonomous navigation in narrow passages.

The authors previously implemented a different method of motion control to solve the same problem [4]. In the previous method, linear velocity is increased based on the difference between the commanded velocity and the actual velocity when wall deadlock is detected. This method has a similar effect to the proposed method in terms of increasing rotation radius as a result. However, the previous method does not directly adjust the rotation radius and several main parameters are manually adjusted based on 'rules of thumb'. The proposed method is directly derived from a dynamics of wall deadlock, and unclear parameters are excluded. The proposed method also derives minimum rotational radius using the information of driving force expected from the motor current. This information is quite important to calculate the minimum rotation radius, but it is not considered in the previous method.

The main contribution of this letter is as follows:

- A method for estimating the minimum rotation radius is constructed based on a dynamics of wall deadlock in order to generate wall-deadlock evasion motion.
- A wall-deadlock evasion process is implemented based on the minimum rotation radius estimation.
- The minimum rotation radius estimation method is tested, and the results show that it can successfully estimate the condition to evade wall deadlock.
- The wall-deadlock evasion method is tested on various floor materials, and it shows higher performance in the reproducibility of motion compared with our previous method [4].

II. RELATED WORK

As shown in Table I, wall deadlock occurs on non-holonomic vehicles with a differential-steering mechanism, while does not occur on ackermann-steering and omni-directional vehicles because they can change the direction of driving force while leaving the wall.

This section describes the related works of wall deadlock evasion for non-holonomic vehicles with a differential-steering mechanism. These approaches can be categorized into several groups. The first one is mechanical solutions, which were used for small-size differential-wheeled [2], [3] vehicles. Meanwhile, the second group includes a control-based solution, which utilize contact with walls for the motion [1]. Moreover, third group includes control methods for collision avoidance [5]–[7] and compliance control [8]–[10], which were considered as solution candidates at the initial stage of our study. However, these solutions were regarded as not suitable for solving the wall deadlock problem on tracked vehicles, due to the detailed reasons described as follows:

There are several reports on mechanical approach for directly dealing with collision. Among them, the simplest solution is the introduction of circular-shaped body applied to Roomba [2], to prevent opposite rotational moment during collision. Another solution is based on the shock-absorbing bumper mechanism [3] to reduce the force that hinders the motion, which is the first approach that focuses on actively utilizing collision on an autonomous mobile robot. Although the objective is similar to these approaches, our proposed method is based on motion control and is advantageous in terms of motion adjustment. In addition, these hardware-based approaches cannot be applied for tracked vehicles with sub-tracks, because they require covering the entire vehicle body, including sub-tracks. Whereas, our proposed method does not require such a major hardware changes.

On the other hand, wall-contacting drive [1] is introduced for a skid-steering vehicle as a control-based solution for the wall deadlock problem, which is proposed for autonomous high-speed transportation vehicle in narrow corridor of underground mining. They developed convexity detection method using laser scanning sensor and implemented wall leaving motion based on the measurement to avoid the wall surface convexity. They also reported that the robot failed to leave the wall in some cases after successful convexity detection, especially in sharp curves. They discussed the difficulty of allowing the robot to turn in a small turning radius to leave the wall in such situation, and claimed that earlier convexity detection is required for larger turning radius. The authors focus more on the motion control using dynamics rather than the convexity detection, because the main problem in such case is that the robot cannot leave the wall even if the wall-leaving motion is commanded. By introducing our proposed method, wall-leaving motion becomes promising because it estimates the minimum rotation radius to realize the motion.

Meanwhile, collision avoidance, or local path planning methods, are actively developed for autonomous mobile robots to prevent failure caused by collisions. The potential method [5] or Vector Field Histogram [6] plan local paths based on virtual force fields by considering the force of attraction from a target and repulsive force from the obstacles. The dynamic window approach [7] is a collision avoidance method directly derived from the dynamics of mobile robots to realize faster locomotion. These methods can generate paths moving away from approaching obstacles and can generate corresponding avoidance motion. However, in the case of industrial plant inspection tasks, the robot cannot avoid all the collisions because of the small margin

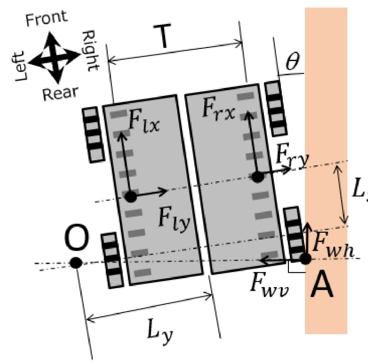

Fig. 3. Dynamics of tracked vehicle during wall deadlock.

to the obstacles and track's slippage during rotational motion. Therefore, it is essential to consider the motion after the robot collides the wall. In such a scenario, collision force obstructs the motion if the robot collides surrounding obstacles so that the robot cannot follow the planned path while moving away from the obstacle. Thus, the authors focus on how to generate desired motion while the vehicle collides the wall.

Compliance control [8]–[10], at the same time, is a major method used for computer-controlled manipulators, which puts a force feedback term in the position control system and adjusts the stiffness of the actuators according to the environment. The method is introduced to realize passive motion to the external force. Based on it, in case of the wall deadlock problem, the robot needs to generate motion in the opposite direction to the external force. However, a problem arises when the robot cannot generate sufficient rotational moment to exceed the opposite moment generated by the collision force, which cannot be solved through stiffness adjustment. The authors construct a new motion control method to actively generate opposite motion to the constraint of collision force.

Several papers have reported the usefulness of external force utilization. Koyanagi *et al.* proposed grasping a handrail while a humanoid robot walks on uneven terrain in order to increase the stability of bipedal motion [11]. Kohanbash *et al.* proposed to use a plow when a tracked vehicle turned on a sandy ground [12]. In case of tracked vehicles for plant inspection, the outer force from the wall was useful for positioning. This study mainly deals with wall deadlock evasion because it is a necessary function in utilizing collision force for motion.

This letter proposes a control method for evading the wall deadlock problem for non-holonomic mobile mechanism.

III. Construction of Wall Deadlock Evasion Control

A. *Modeling of Wall Deadlock*

The main purpose of the modeling is to clarify the condition for generating rotational motion to the target direction. The equation of rotational moment is used for deriving the condition. The equation of linear motion is not described here because it is not used for motion control in the subsequent sections.

Fig. 3 shows a dynamics of a tracked vehicle during wall deadlock. Table II shows parameters of the model. A coordinate frame is fixed on the center of the robot, whose X axis faces front and Y axis faces left. Although the model describes collision on the rear-right corner, it also can be applied to the cases of

TABLE II
PARAMETERS IN DYNAMIC MODEL

F_{rx}	driving force of right track
F_{lx}	driving force of left track
F_{ry}	slide friction force of right track
F_{ly}	slide friction force of left track
F_{wn}	normal force from a wall
F_{wf}	friction force from a wall
T	tread
θ	angle between wall and robot
l_y	distance between center of gravity and collision point in Y-axis
l_x	distance between center of gravity and collision point in X-axis
(L_x, L_y)	location of rotation center on robot coordinate system
μ_g	maximum coefficient of static friction between track and ground
M	robot weight
v	linear velocity of the robot (Longitudinal direction)
ω	angular velocity of the robot

collision on any of the other corners by changing the sign of body size parameters (l_x, l_y).

As a premise, geometrical constraint is introduced as (1) because the collision point A moves on the wall surface.

$$\tan\theta = \frac{l_x + L_x}{l_y + L_y} \tag{1}$$

According to (1), the line OA is vertical to the wall. (2) is introduced because passive wheels are attached on the side surface of the robot as shown in Fig. 1(b).

$$F_{wh} = 0 \tag{2}$$

the equation of rotational moment is shown as (3), based on the model.

$$\tau = F_{rx}\left(L_y + \frac{T}{2}\right) + F_{lx}\left(L_y - \frac{T}{2}\right) - (F_{ry} + F_{ly})L_x \tag{3}$$

In (3), τ is a rotational moment of the robot around rotational center O, and it is positive in the counter clock-wise direction. In this equation, the first and second terms on the right side show a positive moment generated by the driving force of of the motors. (3) does not have terms of collision force because friction force F_{wh} is ignored in (2), and normal force F_{wv} does not have a distance to the rotation center because of the geometrical constraint in (1). The last term of (3) shows a negative moment generated by the lateral friction force. In (3), the controllable parameters are driving force (F_{rx}, F_{lx}) and rotational radius L_y. These can be adjusted by adjusting torque or velocity of the driving motors. Other parameters are fixed or cannot be directly controlled. The robot can rotate to the commanded direction if $\tau > 0$, which means that the positive moment exceeds the negative moment. Here, the condition of rotation is derived as an equation of rotation radius L_y because rotation radius does not have physical limitation, whereas (F_{rx}, F_{lx}) have the limitation that they cannot exceed the static friction force between the floor and the track belt. (4) is derived by substituting $\tau > 0$ into (3).

$$L_y > \frac{(F_{ry} + F_{ly})L_x - \frac{(F_{rx} - F_{lx})T}{2}}{F_{rx} + F_{lx}} \tag{4}$$

In (4), L_y is described as a relationship between the robot's linear velocity v and angular velocity ω as shown in (5).

$$L_y = \frac{v}{\omega} \tag{5}$$

By adjusting the velocity command (v, ω) to satisfy (4), the condition of minimum rotation radius is satisfied in order to generate sufficient rotational moment. These equations are used for determining motion in Section III-B2.

B. Implementation of Wall Deadlock Evasion Control

The authors implemented a wall deadlock evasion process which satisfies the following items:

1) The process can detect wall deadlock and its collision point (front-right, front-left, rear-right or rear-left) by itself.
2) The process only uses inertial sensors such as IMU, motor velocity or motor torque, to make it available to work as a low-level process.

To satisfy these two requirements, the authors implement wall deadlock evasion in two steps, detection and motion adjustment. The equations of the model in Section III-A is mainly used in the latter part. Details of detection and motion adjustment are described in Section III-B1 and Section III-B2, respectively.

1) Detection of Wall Deadlock: First, wall deadlock is detected using the gyroscope sensor and velocity of the tracks. During wall deadlock, actual rotation speed is much lower than the value which is calculated from the track's velocity because the rotational motion is restricted by the wall. The authors therefore introduce angular velocity ratio α as an index of wall deadlock detection as shown in (6).

$$\alpha = \frac{\omega_{\text{track}}}{\omega_{\text{gyro}}} = \frac{V_r - V_l}{T\omega_{\text{gyro}}} \tag{6}$$

In (6), ω_{gyro} is a robot's rotation speed measured by a gyroscope sensor attached to the robot, ω_{track} is a robot‘s rotation speed calculated from both side track's velocity measured by rotary encoders, and T is a tread. (V_r, V_l) are the measured outer velocity of the right and left side tracks, respectively. The authors experimentally found that α is between 1.0 and 1.5 if wall deadlock has not occurred because commanded angular velocity and the actual one should be nearly the same in this case. α will be more than 5.0 if wall deadlock has occurred. The authors implement the wall deadlock detection by monitoring α and fixing a threshold for the index.

After detecting the wall deadlock, the collision point should be identified, whether front-right, front-left, rear-right, or rear-left is colliding. The authors experimentally found that the driving force of the wall-side track is much smaller than the other side track during wall deadlock (the underlying data is described in the appendix). Here, collision side is detected by comparing the driving force of both side tracks using an index, $ForceRatio$, as in (7).

$$ForceRatio = \frac{|F_r| - |F_l|}{|F_r| + |F_l|} \tag{7}$$

Here, $ForceRatio$ is between -1.0 and 1.0 at any moment. This index can be used for detecting which side of the robot collides the wall, as shown in (8).

$$ForceRatio = \begin{cases} x \mid 0 > x \geq -1.0 \text{ (\textbf{if} right collision)} \\ x \mid 0 < x \leq 1.0 \text{ (\textbf{elseif} left collision)} \end{cases} \tag{8}$$

Whether the right side or left side is colliding can be determined using (8). Whether the front or rear is colliding can be detected based on rotation direction. By combining these two pieces of information, the collision point is determined.

2) Motion Command Adjustment During Wall Deadlock: After detecting the collision point, motion command should be adjusted to satisfy (4). In (4), the lateral friction (F_{ry}, F_{ly}) cannot be directly measured. Additionally, L_x cannot be measured under the assumption that no external sensor is used. Thus, the authors assume the most difficult case that θ, the angle between the wall and the robot, is zero, and the maximum friction force is determined as lateral friction, as shown in (9).

$$(F_{ry} + F_{ly})L_x \simeq \mu_g M g l_x \tag{9}$$

By substituting (9) into (4), (10) is derived.

$$L_y > \frac{\mu_g M g l_x - \frac{(F_{rx} - F_{lx})T}{2}}{F_{rx} + F_{lx}} \tag{10}$$

In (10), μ_g, M, g, l_x and T are static values, which can be measured before the robot operation.

The driving force of both side tracks, (F_{rx}, F_{lx}), can be detected from motor torque. Thus, by substituting driving force in every control cycle, the constraint of rotation radius is derived from the equation.

If the commanded motion does not satisfy (10), the set of commanded velocity (v, ω) is adjusted based on (5) and (10). Linear velocity v should be increased to satisfy the equation. In the case that v cannot be increased because of the velocity limitation, ω should be lowered to satisfy the equation.

In (10), the state of the robot is described by only three values, F_{rx}, F_{lx}, and L_y because the other parameters are determined as constants. Thus, the equation is expressed as a three-dimensional diagram as shown in Fig. 4. In this graph, the horizontal axes show the driving force of both side tracks (F_{rx}, F_{lx}), and the vertical axis shows the rotation radius L_y. The curved surface describes the boundary of condition whether the robot can generate sufficient rotational moment or not. During wall deadlock, the state of the robot is described as a point in this space and equation (10) is satisfied if the state is above the boundary plain.

The authors note that (10) and Fig. 4 contains an assumption of static friction in (9) and that might cause a deviation between the model and the phenomenon. It requires an experimental verification that the phenomenon is expressed using (10) and Fig. 4. Experiments are conducted to clarify these points in latter sections.

IV. Evaluation

A. Analysis of Motion During Wall Deadlock

This experiment is conducted to confirm that the wall deadlock can be correctly expressed using Fig. 4. During wall deadlock, the state of the robot is expressed as a point in a diagram

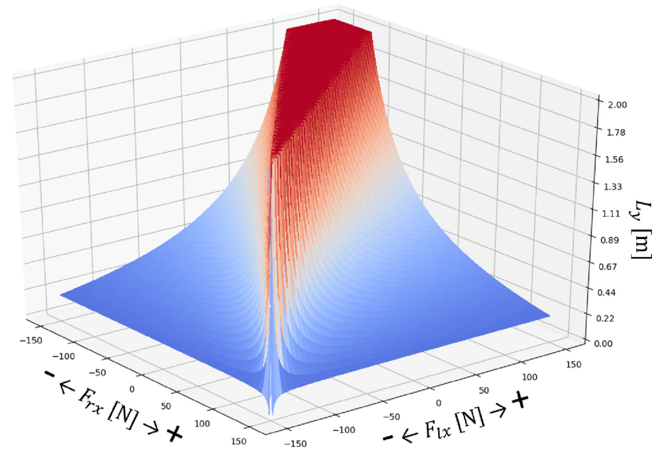

Fig. 4. State diagram of wall deadlock. Horizontal axes show driving force of both side tracks (F_{rx}, F_{lx}), and vertical axis shows rotation radius L_y. A state of the robot is described as a point in this space. equation (10) is satisfied if the state is above the boundary plain.

TABLE III
Conditions for Commanded Velocity. The Experiment is Conducted in Three Levels of Linear Velocity and Four Levels of Angular Velocity. IDs are Assigned for Each Conditions From 1 to 12

		ω[°/s]			
		15	30	45	60
v[m/s]	0.20	1	2	3	4
	0.30	5	6	7	8
	0.40	9	10	11	12

shown in Fig. 4, and it is assumed that the robot can evade wall deadlock if the state is shifted to above the boundary surface.

In this experiment, constant velocity is commanded for five seconds to the robot during wall deadlock, in which the angle between the robot and the wall is 0° in the initial state. The experiment is conducted for multiple conditions of commanded velocity as shown in Table III. Wheel velocity and motor torque are measured during the motion, and the state of the robot is drawn on the diagram based on these measured information. During the motion, the mean angular velocity was measured as an indicator of rotational motion. This experiment is performed on flat wooden floor.

It is assumed that the robot can rotate in the commanded direction if the state satisfies the condition during motion.

B. Performance Verification of Wall Deadlock Evasion

In this experiment, wall deadlock evasion is tested on various floor materials as shown in Fig. 5. At the beginning, the side surface of the robot completely touches the wall. Constant rotational motion (45 °/s) is commanded for the wall deadlock evasion process, and the robot starts to leave the wall. During the motion, robot trajectory is measured using a motion capture camera. Motion is commanded until the angle between the robot and the wall gets more than 90°. Also, acceleration in forward direction is measured using IMU sensor equipped on the robot. The experiment is performed for five times for each condition.

As a result, robot trajectory, mean acceleration during operation, position distribution in endpoint, and operation time are

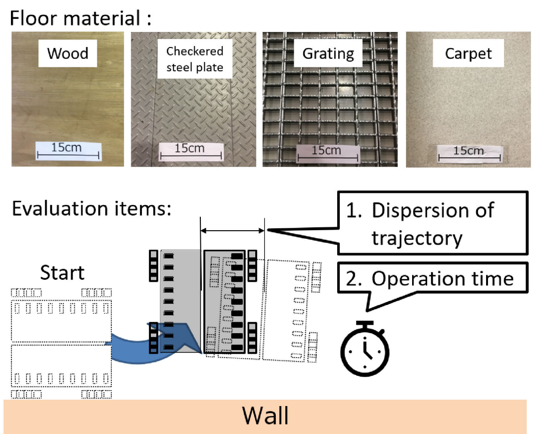

Fig. 5. Experimental setup for evaluation of wall-deadlock evasion. This experiment is conducted on four types of floor materials: wood, grating, checkered steel plate and carpet. A constant rotational motion (45 °/s) is commanded to the robot until the angle between the robot and the wall is more than 90°. the robot's trajectory, mean acceleration, endpoint position, and operation time are measured.

described in Section V. The same experiment is also performed with our previous method [4], to compare the results.

C. Collision Force Measurement During Wall Deadlock Evasion

Collision force is measured during wall deadlock evasion by attaching the force sensor behind the passive wheels in Fig. 1(b). The experiment is performed with our previous method [4] and the proposed method. The experiment is performed five times for each condition. The floor material is wood. Time series data and maximum values are described in Section V.

V. Results

A. Analysis of Motion During Wall Deadlock

Here, two representative results are described using state diagrams as examples: a case that the robot CANNOT rotate and a case that the robot CAN rotate. Other results are described as a ratio of satisfying the condition of (10) during the operation time. Fig. 6 shows the state diagram during wall deadlock in the case that the robot CANNOT rotate. Blue dots show the state translation during operation. It shows that the state is below the boundary plane throughout the operation, which means that (10) is not satisfied at any time. Fig. 7 shows a state diagram during wall deadlock in the case that the robot CAN rotate. It shows that the state is shifted above the boundary plane during the operation, as highlighted by a red circle, which means that (10) is satisfied at those time.

Fig. 8 shows the results of all conditions, which shows the relationship between rotational motion and whether the state satisfies (10). The conditions are ordered according to the mean angular velocity during operation. It clearly shows that the rotation angle is larger when the ratio is larger.

The results show that the robot can rotate to the commanded direction during collision if (10) is satisfied. Thus, it is guaranteed that wall deadlock is avoided if the commanded velocity satisfies (10).

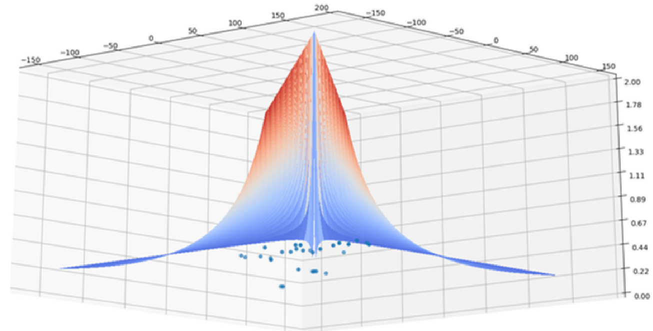

Fig. 6. Representative state diagram when the robot CANNOT rotate during collision. Blue dots show state translation during operation. It shows that the state is below the boundary plane throughout the operation, which means that (10) is not satisfied at any time. The sets of commanded velocity are: $v = 0.20[\mathrm{m/s}], \omega = 60[^\circ/\mathrm{s}]$.

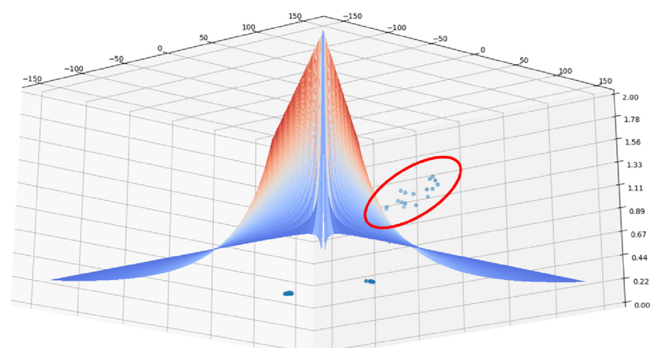

Fig. 7. Representative state diagram when the robot CAN rotate during collision. Blue dots show state translation during operation. It shows that the state is translated above the boundary plane, as highlighted in the red circle, which means that (10) is satisfied at those times. The sets of commanded velocity are: $v = 0.20[\mathrm{m/s}], \omega = 15[^\circ/\mathrm{s}]$.

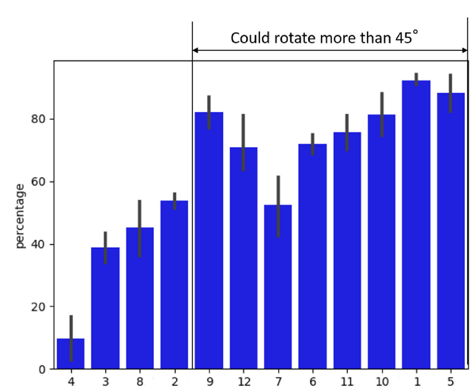

Fig. 8. Relationship between the ratio of satisfying (10) and rotation angle. The bars are ordered by its mean angular velocity during operation. It clearly shows that the rotation angle is larger when the ratio is larger.

B. Performance Verification of Wall Deadlock Evasion

Here, trajectories on a wooden floor are described as examples of motion, and performance on all floor materials are compared with respect to mean acceleration, positioning distribution, and operation time.

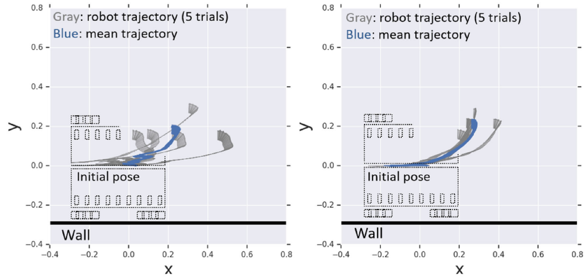

(a) Conventional (b) Proposed

Fig. 9. Comparison of trajectories during wall deadlock evasion. (a) shows results of conventional method [4] and (b) shows those of proposed method. Gray arrows show trajectories of five trials and blue show a mean trajectory. Mean trajectory is calculated by normalizing operation time from zero to one.

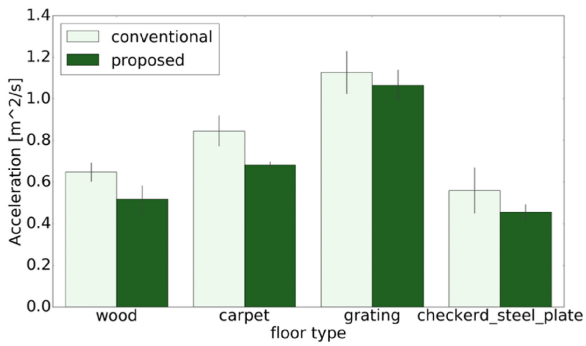

Fig. 10. Comparison of mean acceleration for each floor material. Light green bars show the results of our previous method [4] and dark green show that of the proposed method. Error bars show standard deviation.

Fig. 9(a) shows the trajectory of wall deadlock evasion on a wooden floor using our previous method [4]. Fig. 9(b) shows the trajectory of wall deadlock evasion on a wooden floor using proposed method.

Fig. 10 shows a comparison of mean acceleration for each floor material. Light green bars show the results of our previous method [4] and dark green show that of the proposed method. Error bars show standard deviation. In all the conditions, mean acceleration is significantly smaller in the proposed method.

Fig. 11 shows position distribution at the endpoint of wall-deadlock evasion motion. White bars show the results of our previous method [4] and blue shows that of the proposed method. It shows that position distribution is smaller in the proposed method in all the conditions.

Fig. 12 shows operation time for each trial. Light green bars show the results of our previous method [4] and dark green show that of proposed method. Operation times tend to be smaller in wood, carpet and grating floors, but there is no significant difference.

The results show that the mean value of acceleration and position distribution is smaller in proposed method, which means that reproducibility of motion is improved compared with the conventional method. There are no significant differences in operation time.

C. Collision Force Measurement During Wall Deadlock Evasion

Fig. 13 shows the time-series data of collision force during wall-deadlock evasion. Blue show the results of our previous

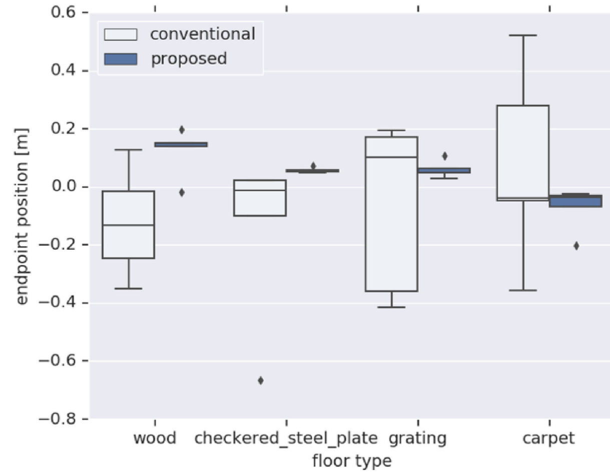

Fig. 11. Position distribution at the endpoint of wall-deadlock evasion motion. White bars show the results of our previous method [4] and blue shows that of the proposed method. The floor types are wood, checkered steel plate, grating and carpet. It shows that position distribution is smaller in proposed method in all the conditions. The position is measured in a parallel direction to the wall (the same as the X-axis in Fig. 9(a) and (b).) The origin of distribution is the endpoint of mean trajectory for each condition.

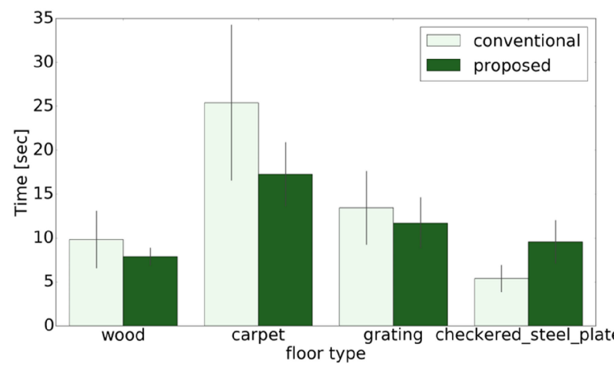

Fig. 12. Operation time for each trial. Light green bars show the results of our previous method [4] and dark green show that of the proposed method. Error bars show standard deviation.

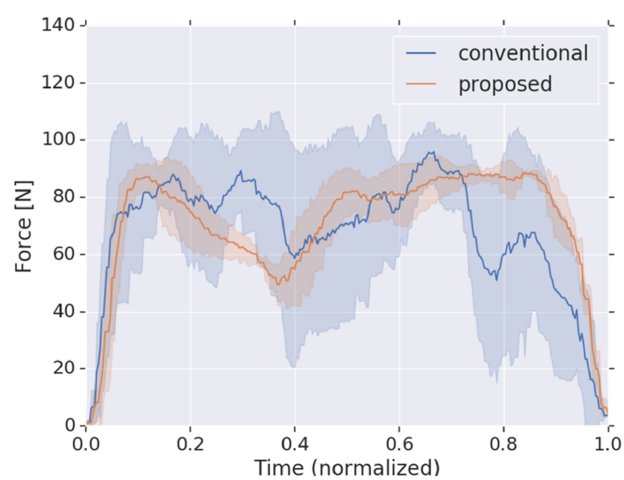

Fig. 13. Time-series data of collision force during wall-deadlock evasion. Blue show the results of our previous method (conventional) [4], Orange show those of proposed method. Time is normalized from 0 to 1 for comparing data with different length. Solid lines show mean value of collision force and band areas show standard deviation.

TABLE IV
COMPARISON OF MAXIMUM COLLISION FORCE DURING OPERATION

	Conventional	Proposed
N	5	5
Mean [N]	104	93.3
SD	6.94	1.70
P-value	0.03	

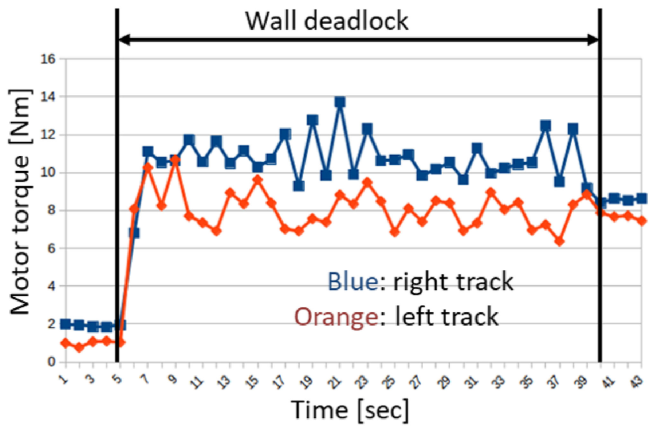

Fig. 14. Biased driving motor torque during wall deadlock. The authors experimentally found that the right side collision or left side collision can be detected by comparing motor torque.

method [4] and Orange shows that of the proposed method. In this figure, time is normalized from 0 to 1 for comparing data of different lengths. The graph shows that the distribution of measured force is smaller in the proposed method, compared with our previous method.

Table IV shows a comparison of maximum force during operation. The maximum force of our previous method is 104[N] in average and that of proposed method is 93[N]. The maximum force is 10% less in the proposed method.

VI. DISCUSSION

In Section V-A, the results showed that the robot can rotate to the commanded direction if (10) is satisfied. This means that (10) successfully predicted the capability of wall-deadlock evasion even when it contains an assumption of static lateral friction as shown in (9). This assumption fixes the shape of the state diagram shown in Fig. 4 and makes it possible to estimate minimum rotational radius L_y using only inertial sensor data. The authors therefore introduced this assumption for implementing the wall-deadlock evasion process.

In Section V-B, the results show that the mean acceleration is significantly decreased in the proposed method, compared with our previous method. The authors assume that the proposed method can estimate minimum rotational radius so that there is no need to drastically change the motion during wall deadlock evasion, whereas the conventional method often involved front-back switching operation. As a result, as shown in Fig. 11, position distribution is also decreased in the proposed method.

In Section V-C, the results show that the variation of collision force is reduced in the proposed method compared with our previous method. Also, the peak value of collision force was 10% less in the proposed method. The authors assume that the reason is the same as that for the position distribution, that the proposed method does not drastically change the motion during operation.

Throughout the results, performance of the proposed method is higher than the conventional method in terms of reproducibility of motion and smaller collision force.

VII. CONCLUSION

In this letter, the authors constructed a wall-deadlock evasion method based on rotation radius adjustment. Based on the model of wall deadlock as shown in Fig. 3, the condition of minimum rotation radius is estimated by (10). This formula can be expressed as a state diagram as shown in Fig. 4. Experimental results show that it is possible to identify whether the robot can evade wall deadlock using (10). Wall deadlock evasion process is implemented using the formula and tested on various floor surfaces. The results show that the proposed method has higher performance compared with a conventional method in terms of reproducibility of motion and smaller collision force during operation.

In Section III-B1, the authors introduced $ForceRatio$ in (7) as an index of collision point detection. As shown in Fig. 14, the authors experimentally found that driving motor torque is biased during wall deadlock, and the torque of the wall side motor is always smaller than that of the other side. By using this information, the collision side is detected before starting wall-deadlock evasion.

REFERENCES

[1] H. Karasawa, T. Okubo, R. Fukui, M. Nakao, and Y. Kodama, "High-speed wall-contacting drive for underground automatic transport vehicle," in *Proc. Int. Symp. Exp. Robot.*, 2017, vol. 1, pp. 367–373.
[2] J. L. Jones, "Robots at the tipping point: The road to iRobot Roomba," *IEEE Robot. Autom. Mag.*, vol. 13, no. 1, pp. 76–78, Mar. 2006.
[3] M. Rude, "A flexible, shock-absorbing bumper system with touch-sensing capability for autonomous vehicles," in *Proc. IEEE/RSJ Int. Conf. Intell. Robots Syst.*, 1996, vol. 2, pp. 410–417.
[4] S. Kojima, K. Ohno, T. Suzuki, T. Westfechtel, Y. Okada, and S. Tadokoro, "Motion control of tracked vehicle based on contact force model," in *Proc. IEEE/RSJ Int. Conf. Intell. Robots Syst.*, 2016, pp. 1177–1183.
[5] R. C. Arkin, *Motor Schema - Based Mobile Robot Navigation*, vol. 8. Thousand Oaks, CA, USA: Sage, 1989, pp. 92–112.
[6] J. Borenstein and Y. Koren, "The vector field histogram - fast obstacle avoidance for mobile robots," *IEEE Trans. Robot. Autom.*, vol. 7, no. 3, pp. 278–288, Jun. 1991.
[7] D. Fox, W. Burgard, and S. Thrun, "The dynamic window approach to collision avoidance," *IEEE Robot. Autom. Mag.*, vol. 4, no. 1, pp. 23–33, Mar. 1997.
[8] M. T. Mason, "Compliance and force control for computer controlled manipulators," *IEEE Trans. Syst., Man, Cybern.*, vol. SMC-11, no. 6, pp. 418–432, Jun. 1981.
[9] K. S. Kim, A. S. Kwok, G. C. Thomas, and L. Sentis, "Fully omnidirectional compliance in mobile robots via drive-torque sensor feedback," in *Proc. IEEE/RSJ Int. Conf. Intell. Robots Syst.*, 2014, pp. 4757–4763.
[10] J. K. Salisbury, "Active stiffness control of a manipulator in cartesian coordinates," in *Proc. 19th IEEE Conf. Decis. Control Including Symp. Adaptive Processes*, 1980, vol. 19, pp. 95–100.
[11] K. Koyanagi *et al.*, "A pattern generator of humanoid robots walking on a rough terrain using a handrail," in *Proc. IEEE/RSJ Int. Conf. Intell. Robots Syst.*, 2008, pp. 2617–2622.
[12] D. Kohanbash, S. Moreland, and D. Wettergreen, "Plowing for rover control on extreme slopes," in *Field and Service Robotics*. Berlin, Germany: Springer, 2014, pp. 399–413.